PROCEEDINGS OF ECOS 2023 - THE 36TH INTERNATIONAL CONFERENCE ON
EFFICIENCY, COST, OPTIMIZATION, SIMULATION AND ENVIRONMENTAL IMPACT OF ENERGY SYSTEMS
25-30 JUNE, 2023, LAS PALMAS DE GRAN CANARIA, SPAIN

Integrated design and operation optimization of multi-energy systems including energy networks

Enrico Dal Cin[a], Gianluca Carraro[b], Andrea Lazzaretto[c], George Tsatsaronis[d], Gabriele Volpato[e], and Piero Danieli[f]

[a] *University of Padova, Industrial Engineering Department, Padova, Italy, enrico.dalcin@phd.unipd.it, CA*
[b] *University of Padova, Industrial Engineering Department, Padova, Italy, gianluca.carraro@unipd.it*
[c] *University of Padova, Industrial Engineering Department, Padova, Italy, andrea.lazzaretto@unipd.it*
[d] *Technische Universität Berlin, Chair of Energy Engineering and Environmental Protection, Berlin, Germany, georgios.tsatsaronis@tu-berlin.de*
[e] *University of Padova, Industrial Engineering Department, Padova, Italy, gabriele.volpato.1@phd.unipd.it*
[f] *University of Padova, Department of Management and Engineering, Vicenza, Italy, piero.danieli@unipd.it*

Abstract:

A multi-energy system is composed of four main subsystems: i) energy conversion, ii) energy transportation, iii) energy supply, and iv) energy storage. Recent works in the literature dealing with the design and operation optimization of multi-energy systems usually include only one of the above-mentioned subsystems at a time and neglect the others or consider them as constraints imposed a priori. That kind of approach may lead to near optimal system configurations. In fact, the global optimum can only be achieved by the synthesis, design and operation optimization of the system in its entirety. Here, a mixed integer linear programming (MILP) approach is proposed to simultaneously optimize the size of the energy conversion and storage plants, the capacity of the energy networks, and the operation of the whole multi-energy system. The objective function consists in minimizing the life cycle cost of the system while imposing an upper bound on greenhouse gas emissions. Moreover, this upper bound can be iteratively reduced to consider increasingly stricter decarbonization targets. A district composed of commercial and residential buildings, with their own electricity and heating demands and operating in a microgrid, is considered as a case study. Heat is provided to the end users via a district heating network, while electricity can be either generated on site or imported from the national grid. Results shows a reduction potential in carbon emissions of 45% for the considered system, together with an 8% reduction of the life cycle cost, with respect to a reference scenario.

Keywords:

Decarbonization; District heating; Microgrid; Multi-energy systems; Optimization.

1. Introduction

The increasing threat of climate change requires timely interventions to drastically reduce the anthropogenic emissions of greenhouse gases By accounting for 75% of the global carbon emissions, the energy sector is the main responsible of global warming. However, the increasing availability at low cost of energy conversion technologies based on Renewable Energy Sources (RES) can pave the way to a deep decarbonization process. To this scope, fostering the distributed generation, electrifying the energy consumption and exploiting the synergies between different final energy sectors, as, for instance, the electricity and heating ones, can play a crucial role in improving the penetration of RES while decreasing the consumption of fossil fuels [1]. All these actions contribute to the development of Multi-Energy Systems (MESs).

A MES is defined as an energy system of any spatial extent (a single building, a district, a city, a nation, …) that involves different types of energy carriers (electricity, heat, fossil fuels, biomass, …) and provide energy in various forms to the end users [2]. It is composed of four main subsystems.

1. Energy conversion. The fleet of the energy conversion plants that provides the end users with the required energy in the required forms.

https://doi.org/10.52202/069564-0302

2. Energy transportation. The energy networks collecting energy from the conversion plants and delivering it to the end users.
3. Energy supply. The end users of the system with their specific energy demands.
4. Energy storage. Components that allow storing energy in different forms in a certain moment and delivering it in a later one. They can be integrated at any level (energy conversion, transportation, supply).

A holistic approach to the study of MESs should consider all the above-mentioned aspects. Thus, the complete optimization of a MES accordingly to a certain objective function should involve three levels of analysis.

1. Synthesis, which targets the topology of the energy networks and the number, type and location within the system of the energy conversion and storage plants required to fulfil the energy demands of the end users.
2. Design, which targets the sizing of the energy conversion and storage plants and the capacity of each branch of the energy networks.
3. Operation, which targets the management of the dispatchable plants, the management of the power and mass flows within the networks, and the application of eventual demand response strategies [3].

Such kind of optimization problems, referred to as Synthesis, Design and Operation (SDO) optimization, is the most complete in the field of energy systems, but also the most challenging to solve, due to the high number of decision variables, either continuous or integer/binary [4].

This paper focuses on MESs at the district level including microgrids and district heating networks (DHNs). An increasing number of works in the recent literature deals with the optimization of such kind of systems. However, most of those works do not embrace a holistic approach but focus on a specific optimization problem (synthesis, design, operation) or a specific aspect of the MES (energy conversion, storage, transportation, supply).

Integrated district energy networks were studied by several authors. Lund et al. [5] highlighted the importance of integrating different energy networks (e.g., district heating, electricity distribution and natural gas supply) at the district level to shape the smart energy system of the future. In this context, decreasing the supply temperature of DHNs (e.g., with 4th and 5th generation DHNs) can facilitate the integration of RES, power to heat technologies and other smart energy systems (e.g., microgrids). Leitner et al. [6] stated that the components required to build up smart energy systems are well known and already available in the market, whereas there is a lack of analyses at a system level. Their study focuses on a modelling and simulation approach for coupled district heating and electrical distribution networks. The DHN is defined by a dynamic thermal-hydraulic model, whereas the electrical distribution network by a quasi-static model. The model is complete but does not involve any kind of optimization, which would probably result in a computational intractability. Other authors, e.g., Nazari-Heris et al. [7], studied the optimal operation of highly integrated MESs involving many energy or energy-related networks (e.g., electricity, heating, natural gas and water networks). However, these models are computationally expensive (they are typically applied to one-day operation) and cannot be applied to the design optimization of those networks. Talebi et al. [8] reviewed the optimization approaches to the design of DHNs and highlighted the relevant role that optimization tools can have in designing district energy systems integrating a high share of RES and energy storage technologies. Moreover, they found out that the most used design optimization techniques are based on numerical approaches, as Mixed Integer Linear or Non-Linear Programming (MILP and MINLP, respectively), or meta-heuristic approaches, as evolutionary or genetic algorithms. Röder et al. [9] developed a MILP optimization framework for the SDO optimization of a DHN. They considered a mixed residential-commercial district in Germany and searched for the cost-optimal topology, capacity, and operation of the DHN supplying all the users of the district. However, they did not optimize the generation and storage sides of the system as they fixed in advance the position, type and capacity of the energy conversion and storage plants providing the network with the required heat, and they did not consider the electricity network.

On the other hand, many authors focused on the optimal design and/or operation of the energy conversion and storage plants supplying a district MES. Rech et al. [10] studied the optimal operation of a fleet of energy conversion plants providing electrical and thermal energy to a mountain village. Heat is generated by means of biomass-fuelled boilers or combined heat and power (CHP) plants, and delivered to the end users via DHN, which is modelled as a black box collecting heat from the generators to fulfil the aggregated heating demand of the village. Ghilardi et al.[11] developed a MILP model for the operation optimization of a University campus MES involving a district heating/cooling network and the thermal management of buildings. They found out considerable advantages in terms of cost reduction, energy saving and integration of RES thanks to the optimal management of the thermal comfort in buildings, the optimal dispatch of the available energy conversion systems and the optimal management of the temperature levels of the district heating/cooling network. In a previous work [12], the authors of the present paper proposed a method for the design and operation multi-objective optimization (economical and environmental) of the energy conversion and storage plants providing electricity and heat to an energy community. Demand response was also applied, but no district energy networks were modelled, assuming that the community members directly interface with the national power grid and fulfil their heating demand autonomously. Wirtz [13] proposed a web tool for the optimal conceptual design

https://doi.org/10.52202/069564-0302

of a district MES generation mix. By means of a Linear Programming (LP) approach, the proposed tool allows defining the optimal size of the energy conversion and storage plants available in an energy hub fulfilling the electricity, heating and cooling demands of the district. Heating and cooling can be also provided via district heating and/or cooling networks. Wirtz et al. [14] also proposed a model for the optimal planning of a 5th generation district heating and cooling network. This model optimizes the design (i.e., the size) of the energy conversion and storage plants available at two levels: i) the energy hub and ii) the end users' buildings, which interface with the heating and cooling network by means of heat pumps and chillers. As a last example, Mashayekh et al. [15] developed an optimization tool for the design of the energy conversion and storage plants supplying a multi energy microgrid involving both electricity and heating networks. The optimization addresses the generation mix selection and sizing, the resource siting and allocation, and the operation scheduling. They found out that considering the spatial distribution of a MES, modelled as a multi nodal system, allows a more realistic assessment of the generation portfolio, which can be otherwise non-optimal if the same system is modelled as a single node.

A lack emerges. On one hand, works dealing with modelling of energy networks either neglect the design of energy conversion and storage systems or build complex models that are not suitable for design optimization procedures. On the other hand, works dealing with design-operation optimization of MESs do not consider the optimization of the topology and capacity of the district energy networks, which are considered only as constraints.

A pioneering work about the SDO optimization of a district MES was proposed by Mehleri et al. [16] and further developed in [17]. In these works, a MILP framework is introduced to optimize the selection (capacity and allocation) and operation of the distributed energy conversion plants supplying the district MES, but also the design (topology and capacity) of a DHN connecting the buildings. However, the weakness of the proposed approach is that the DHN is defined by a set of direct heat exchange connections between two buildings that follow the path of minimum "geometrical distance" (i.e., the straight line connecting two buildings). This is a strong simplification because obstacles that can interrupt the path between two buildings are not considered. A more reliable approach in the design of a network should consider the "geographical distance" between nodes, i.e., the "real" path that a network branch must follow to connect two nodes. Accordingly, a typical approach to DHN design (see, for instance, in [9]) consists in constraining pipelines to follow pre-determined paths, which are usually the streets of the district.

To overcome the above-mentioned weaknesses, this work proposes a holistic MILP approach for the optimal design and operation of a district MES, modelled as a multi-nodal system. The goal consists in finding the size of the available energy conversion and storage plants, the capacity of each branch of the available energy networks, and the operation of the whole system that minimize the life cycle cost of the MES, while fulfilling the energy demands of the end users. Moreover, an environmental constraint is imposed on the maximum amount of carbon dioxide (CO_2) emissions. By iteratively decreasing the value of this constraint, a sort of multi-objective optimization can be carried out, in order to obtain the Pareto front of the cost-optimal system configurations that meet increasingly stricter decarbonization targets. A district located in Padova, Italy, composed of commercial and residential buildings with their own electricity and heating demands, and operating in a microgrid is considered here as a case study to highlight the potentiality of the proposed approach. Heat is provided to consumers via DHN, while electricity can be either generated on site or imported from the national grid.

The novelty introduced in this paper consists in proposing a holistic and integrated method for the design and operation optimization of both conversion/storage plants and energy networks of a MES, while maintaining an accurate representation of the networks, which are modelled with the "geographical distance" criterion, instead of the simplified "minimum geometrical distance" one.

Note that the synthesis problem, i.e., the definition of the topology of the networks and of the number, type and position within the system of the energy conversion and storage plants, is not addressed here. Conversely, the topological data are provided as input to the model. However, the proposed approach is intended as a sub-problem of a wider optimization method that addresses the synthesis problem too, in order to provide a complete SDO optimization tool for district MESs. The idea is to implement the overall SDO problem by means of a two-level evolutionary algorithm, in which the first level deals with the synthesis problem. The topology of the system defined in the first level is then passed to the second level, which deals with the design and operation sub-problem (i.e., the model proposed here). Since the design and operation sub-problem must be run several times for each iteration of the evolutionary algorithm, it must be maintained as simple as possible in order to avoid computational intractability. For this reason, the model presented here is maintained linear by means of proper simplifications of the characteristic curves of the technologies and cost data. A similar two-level approach for the SDO of a district heating system with distributed CHP plants was developed by Casisi et al. [18]. However, they only consider DHN and not the electrical network, and they assume a given topology of the DHN.

The rest of the paper is structured as follows. Section 2 presents the case study, while section 3 presents the developed optimization method. Section 4 discusses the results and, finally, section 5 draws the conclusions.

2. Case study

The case study considers a small mixed residential-commercial district located in Padova, Italy. The district is composed of five buildings (end users), with their own electricity and heating demands, and operates in an autonomous microgrid connected to the national power grid. Heat is provided to the end users via DHN, while electricity can be either generated on site or imported from the national grid. The system is modelled as a multi-nodal MES with 16 nodes in total. Figure 1 shows the layout of the considered system. The buildings located at nodes 3, 5 and 15 are residential buildings, the remaining two (nodes 9 and 11) are commercial buildings. Each building owns a photovoltaic plant (PV) and an electrical energy storage (EES) based on lithium batteries. An energy hub located at node 7 and including a gas-fuelled CHP internal combustion engine (ICE), a gas boiler (BOIL), an air-water heat pump (HP) and a thermal energy storage (TES) feeds the DHN that delivers the required heat to the end users. To maintain the model linear, the operating parameters of the networks are fixed a priori and assumed to remain constant during the operation, as in [9]. This simplification allows modelling the networks by considering only the power or heat flows circulating inside them. The supply and return temperatures of the DHN are set at 70°C and 40°C, respectively. The microgrid voltage is 380V.

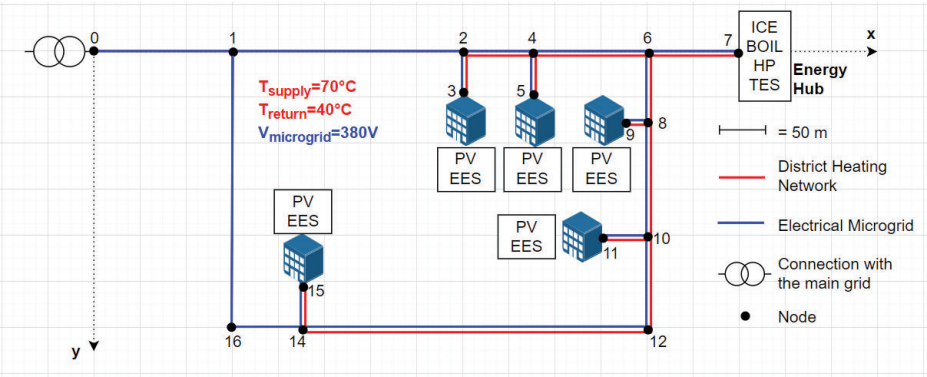

Figure 1 Layout of the multi-energy system considered as case study. The white rectangles contain the conversion and storage plants available at the node where they are located.

The topology of the energy networks can be derived from a geographical map of the district, where the available paths for the network branches are the streets. Accordingly, the layout of the DHN is designed by considering the tree path of "minimum geographical distance" connecting the energy hub to all the end users. In other words, the overall length of the pipelines is minimized, with the constraint of following only the available paths. The same holds true for the electrical microgrid, apart from the inclusion of node 0, which allows the power exchange with the national grid, and the inclusion of the branches between nodes 0-1, 1-2, 2-16 and 14-16, which define a network ring that increases the system reliability.

Table 1 shows the yearly electricity and heating demands of the end users (integral over one year of the hourly demands) and the corresponding demand peaks occurring during the year (maximum values reached by the hourly demands). Since one hour is the time resolution of the model, hourly demands are expressed in unit of power (kW).

Table 1 Yearly electricity and heating demands ($D_{el,year}$ and $D_{th,year}$, respectively) of each end user and aggregated, with the associated demand peaks over the year ($D_{el,peak}$ for electricity, and $D_{th,peak}$ for heating).

Node	$D_{\mathrm{el,year}}$, MWh	$D_{\mathrm{th,year}}$, MWh	$D_{\mathrm{el,peak}}$, kW	$D_{\mathrm{th,peak}}$, kW
3	89.77	73.54	25.0	60.0
5	125.68	98.06	35.0	80.0
9	175.42	20.76	70.0	60.0
11	125.30	17.30	50.0	50.0
15	143.63	122.57	40.0	100.0
Aggregated	659.80	332.23	176.3	344.4

3. Method: MILP optimization

The MILP optimization problem can be formulated in a general form as in Eq. (1) [19].

$$min_{x,y}\{f(\boldsymbol{x},\boldsymbol{y}) = \boldsymbol{c}^T\boldsymbol{x} + \boldsymbol{d}^T\boldsymbol{y}\}$$
$$subject\ to\ \boldsymbol{A}\boldsymbol{x} + \boldsymbol{B}\boldsymbol{y} = \boldsymbol{b} \quad (1)$$
$$with\ \boldsymbol{x} \geq 0 \in \Re^{N_x}, \boldsymbol{y} \in \{1,0\}^{N_y}.$$

https://doi.org/10.52202/069564-0302

f is the objective function, $\boldsymbol{c}$ and $\boldsymbol{d}$ are the cost vectors associated with the continuous and binary variables, $\boldsymbol{x}$ and $\boldsymbol{y}$, respectively; $\boldsymbol{A}$ and $\boldsymbol{B}$ are the constraint matrices and $\boldsymbol{b}$ is the vector of the known terms; N_x and N_y indicate the dimension of $\boldsymbol{x}$ and $\boldsymbol{y}$, respectively.

The considered MES is modelled as a multi-nodal system, with $N = 16$ nodes. In the next sections, the constraints, decision variables and objective function of the problem are introduced. The decision variables are highlighted in bold. The subscript $n = 1,2, \dots, N$ refers to the nodes, $k = 1,2, \dots, K$ to the typical days (or cluster centers), and $h = 1,2, \dots, 24$ to the hours of the day. The optimization model has been developed in Python and solved with the Gurobi solver.

3.1. Time series aggregation

To be solved, the proposed optimization model requires some time series as input. These are i) the electricity demand of each final user, ii) the heating demand of each final user, iii) the global solar irradiation on the horizontal plane, necessary for calculating the PV generation, and iv) the temperature of the ambient air, necessary for calculating the electrical power consumption of the HP. These time series are available for a reference year subdivided in days with an hourly resolution, for a total of $24 \times 365 = 8760$ timesteps for each time series. However, including the time series in their entirety into the optimization model would result in a computational intractability. In fact, the number of decision variables required to solve the operation problem is proportional to the total number of timesteps. Thus, it is necessary to reduce the total number of timesteps and, in turn, the computational burden.

Following Hoffmann et al. [20], a K-medoids clustering approach is applied here to aggregate time series into typical days, which must be representative of the entire year. The chosen number of typical days is eight. Moreover, the two days of the year having the maximum peak value in i) aggregated electricity demand and ii) aggregated heating demand are added to the clustering process as new cluster centers. Thus, the final number of typical days is $K = 10$. Neglecting the extreme peak periods in defining typical days would lead to underestimate the size of the energy conversion plants, which could not meet the extreme demand peaks occurring during the year. The hourly resolution of the time series is preserved, being each typical day composed of $H = 24$ time steps. In this way, the number of decision variables associated with the operation, proportional to the total number of timesteps, is drastically reduced. In fact, the total number of timesteps is diminished from 8760 to $H \times K = 240$. The time series aggregation also returns the weight w_k of each typical day k (with $k = 1,2, \dots, K$), which corresponds to the number of days of the year represented by that typical day. The Python package "*tsam*" has been utilized for time series aggregation.

3.2. Energy conversion and storage systems

The energy conversion plants are modelled according to [21], the energy storage systems according to [22].

3.2.1. Photovoltaic plant

The electrical power (P_{PV}) generated by a photovoltaic plant, in kW, is given by Eq. (2).

$$P_{PV,n,k,h} = \boldsymbol{C_{PV,n}} \frac{I_{sun,k,h}}{I_{sun,ref}}. \quad (2)$$

$\boldsymbol{C_{PV}}$ is the capacity of the PV plant in kW of peak (kW_p) and is a decision variable, I_{sun} is the global solar irradiation in W/m^2 and is provided as a time series, $I_{sun,ref} = 1000\text{W/m}^2$ is the global solar irradiation in the reference conditions in which the kW_p is defined. It is assumed that 1 kW_p of PV requires 7 m^2 of area.

The PV capacity is bounded in between a minimum value, corresponding, for instance, to the area of a single PV module, and maximum one, corresponding to the entire available area at a node, as reported in Eq. (3).

$$C_{PV,min,n} \leq \boldsymbol{C_{PV,n}} \leq C_{PV,max,n}. \quad (3)$$

If PV is not available at the node n, then $C_{PV,min,n} = C_{PV,max,n} = 0$ and, in turn, $\boldsymbol{P_{PV,n,k,h}} = 0$.

3.2.2. Gas-fuelled internal combustion engine in combined heat and power mode

The fuel (natural gas) consumption (F_{ICE}) of the CHP internal combustion engine (ICE), in kW, and its thermal power (Q_{ICE}), also in kW, are given by Eq. (4) and Eq. (5), respectively, as a linear function of the engine power.

$$F_{ICE,n,k,h} = \boldsymbol{P_{ICE,n,k,h}}\alpha + \boldsymbol{\delta_{ICE,n,k,h}}\beta. \quad (4)$$

$$Q_{ICE,n,k,h} = \boldsymbol{P_{ICE,n,k,h}}\rho + \boldsymbol{\delta_{ICE,n,k,h}}\sigma. \quad (5)$$

$\boldsymbol{P_{ICE}}$ is the electric power in kW and is a decision variable, $\boldsymbol{\delta_{ICE}}$ is a binary decision variable equal to 1 if the ICE is working and equal to 0 otherwise. The linearization coefficients of the ICE characteristic curves are $\alpha = 2.42$, $\beta = 11.0\text{kW}$, $\rho = 1.24$, $\sigma = -1.65\text{kW}$.

The capacity $\boldsymbol{C_{ICE}}$ of the ICE, in kW of nominal electric power, which is a decision variable, is associated with the auxiliary decision variable $\boldsymbol{\vartheta_{ICE}}$ in order to avoid nonlinear constraints [23] of the type $\boldsymbol{P_{ICE}} \leq \boldsymbol{C_{ICE}}\boldsymbol{\delta_{ICE}}$. Equations (6), (7), and (8) bound $\boldsymbol{C_{ICE}}$ and $\boldsymbol{P_{ICE}}$.

$$\boldsymbol{\delta_{ICE,n,k,h}} C_{ICE,min,n} \leq \boldsymbol{\vartheta_{ICE,n,k,t}} \leq \boldsymbol{\delta_{ICE,n,k,h}} C_{ICE,max,n}. \quad (6)$$

$$\left(1 - \boldsymbol{\delta_{ICE,n,k,h}}\right) C_{ICE,min,n} \leq \boldsymbol{C_{ICE,n}} - \boldsymbol{\vartheta_{ICE,n,k,h}} \leq \left(1 - \boldsymbol{\delta_{ICE,n,k,h}}\right) C_{ICE,max,n}. \quad (7)$$

$$\gamma_{ml,ICE} \boldsymbol{\vartheta_{ICE,n,k,h}} \leq \boldsymbol{P_{ICE,n,k,h}} \leq \boldsymbol{\vartheta_{ICE,n,k,h}}. \quad (8)$$

$\gamma_{ml,ICE} = 0.7$ is the ratio between the minimum load at which the ICE can operate and its nominal capacity, and $C_{ICE,min}$ and $C_{ICE,max}$ are the minimum and maximum bounds of the ICE capacity, respectively. If the ICE is not available at the node n, then $C_{ICE,min,n} = C_{ICE,max,n} = 0$ and, in turn, $\boldsymbol{P_{ICE,n,k,h}} = \boldsymbol{F_{ICE,n,k,h}} = \boldsymbol{Q_{ICE,n,k,h}} = 0$.

3.2.3. Gas boiler

The fuel (natural gas) consumption (F_{BOIL}) of the gas boiler (BOIL), in kW, is given in Eq. (9) as a function of the thermal power ($\boldsymbol{Q_{BOIL}}$), in kW, which is a decision variable.

$$F_{BOIL,n,k,h} = \frac{\boldsymbol{Q_{BOIL,n,k,h}}}{\eta_{th,BOIL}}. \quad (9)$$

$\eta_{th,BOIL} = 0.9$ is the boiler efficiency. Equations (10) and (11) bound the thermal power ($\boldsymbol{Q_{BOIL}}$) and the boiler capacity ($\boldsymbol{C_{BOIL}}$), expressed in kW of nominal thermal power, which is another decision variable.

$$C_{BOIL,min,n} \leq \boldsymbol{C_{BOIL,n}} \leq C_{BOIL,max,n}. \quad (10)$$

$$0 \leq \boldsymbol{Q_{BOIL,n,k,h}} \leq \boldsymbol{C_{BOIL,n}}. \quad (11)$$

$C_{BOIL,min,}$ and $C_{BOIL,max}$ are the minimum and maximum bounds of the boiler capacity, respectively. If the boiler is not available at the node n, then $C_{BOIL,min,n} = C_{BOIL,max,n} = 0$ and, in turn, $\boldsymbol{F_{BOIL,n,k,h}} = \boldsymbol{Q_{BOIL,n,k,h}} = 0$.

3.2.4. Air-water heat pump

The electric power consumption (P_{HP}) of the heat pump (HP), in kW, is given in Eq. (12) as a function of the thermal power ($\boldsymbol{Q_{HP}}$), in kW, which is a decision variable.

$$P_{HP,n,k,h} = \frac{1}{COP_{ideal,k,h}} \left(\boldsymbol{Q_{HP,n,k,h}}\mu + \boldsymbol{\delta_{HP,n,k,h}}\omega\right). \quad (12)$$

$\boldsymbol{\delta_{HP}}$ is a binary decision variable equal to 1 if the HP is working and equal to 0 otherwise, $\mu = 1.80$ and $\omega = 2.65$kW are the linearization coefficients of the HP characteristic curves (similarly to the ICE), COP_{ideal} is the coefficient of performance calculated in ideal conditions (Carnot equation) between the ambient temperature T_{amb}, in K, provided as a time series, and the supply temperature T_{supply} of the DHN, in K. Equation (13) shows the ideal coefficient of performance.

$$COP_{ideal,k,h} = \frac{1}{1 - \frac{T_{amb,k,h}}{T_{supply}}}. \quad (13)$$

The capacity ($\boldsymbol{C_{HP}}$) of the HP is a decision variable expressed in kW of nominal thermal power, and is associated with the auxiliary decision variable $\boldsymbol{\vartheta_{HP}}$ to avoid nonlinear constraints. Equations (14), (15), and (16) bound $\boldsymbol{C_{HP}}$ and $\boldsymbol{Q_{HP}}$.

$$\boldsymbol{\delta_{HP,n,k,h}} C_{HP,min,n} \leq \boldsymbol{\vartheta_{HP,n,k,h}} \leq \boldsymbol{\delta_{HP,n,k,h}} C_{HP,max,n}. \quad (14)$$

$$\left(1 - \boldsymbol{\delta_{HP,n,k,h}}\right) C_{HP,min,n} \leq \boldsymbol{C_{HP,n}} - \boldsymbol{\vartheta_{HP,n,k,h}} \leq \left(1 - \boldsymbol{\delta_{HP,n,k,h}}\right) C_{HP,max,n}. \quad (15)$$

$$\gamma_{ml,HP} \boldsymbol{\vartheta_{HP,n,k,h}} \leq \boldsymbol{Q_{HP,n,k,h}} \leq \boldsymbol{\vartheta_{HP,n,k,h}}. \quad (16)$$

$\gamma_{ml,HP} = 0.5$ is the ratio between the minimum load at which the HP can operate and its nominal capacity. $C_{HP,min,}$ and $C_{HP,max}$ are the minimum and maximum bounds of the HP capacity, respectively. If the HP is not available at the node n, then $C_{HP,min,n} = C_{HP,max,n} = 0$ and, in turn, $\boldsymbol{P_{HP,n,k,h}} = \boldsymbol{Q_{HP,n,k,h}} = 0$.

3.2.5. Energy storage systems

The decision variables associated with the thermal energy storage (TES) are its capacity ($\boldsymbol{C_{TES,n}}$), in kWh, the charging heat ($\boldsymbol{Q_{TES,chrg,n,k,h}}$) and discharging heat ($\boldsymbol{Q_{TES,disch,n,k,h}}$), in kW, and the state of charge ($\boldsymbol{SOC_{TES,n,h,k}}$), in kWh. The decision variables associated with the electrical energy storage (EES) are its capacity ($\boldsymbol{C_{EES,n}}$), in kWh, the charging power ($\boldsymbol{P_{EES,chrg,n,k,h}}$) and discharging power ($\boldsymbol{P_{EES,disch,n,k,h}}$), in kW, and the state of charge ($\boldsymbol{SOC_{EES,n,h,k}}$), in kWh. Refer to [22] for the model of energy storage systems. Note that both intra-day and inter-

https://doi.org/10.52202/069564-0302

day storage is allowed. If a storage system is not available at node n, then all the corresponding decision variables are set equal to zero.

3.2.6. Electricity import from/export to the national power grid

The microgrid interfaces with the national power grid at node 0. Here, it is possible to import/export electricity. Thus, two additional sets of decision variables are required: $\boldsymbol{P_{imp,n,k,h}}$, in kW, for import, and $\boldsymbol{P_{exp,n,k,h}}$, in kW, for export. $\boldsymbol{P_{imp,n,k,h}} = \boldsymbol{P_{imp,n,k,h}} = 0$ if $n \neq 0$.

3.3. Energy networks

The system includes $P = 12$ district heating pipelines, and $L = 16$ electrical microgrid lines.

3.3.1. District heating network

For each pipeline p (with $p = 1,2, \dots, P$) connecting two nodes n and m, the decision variables involved in the model of the district heating network (DHN) are: the capacity of the pipeline ($\boldsymbol{C_{DHN,p,nm}}$) connecting the two nodes, in kW, the heat flow from node n to node m ($\boldsymbol{Q_{DHN,nm}}$), in kW, and the heat flow from node m to node n ($\boldsymbol{Q_{DHN,mn}}$), in kW. The heat flows are bounded by the pipeline capacity, as shown in Eq. (17).

$$\boldsymbol{Q_{DHN,nm,k,h}} + \boldsymbol{Q_{DHN,mn,k,h}} \leq \boldsymbol{C_{DHN,p,nm}}. \quad (17)$$

Note that, due to the DHN layout (see Figure 1), heat is constrained to flow from the energy hub (node 7) to the end users (nodes 3, 5, 9, 11, 15). Thus, for each pipeline, the flow in one of the two directions is always zero. If two nodes n and m are not connected by a DHN pipeline, then $\boldsymbol{C_{DHN,p,nm}}$ is not defined, and $\boldsymbol{Q_{DHN,nm,k,h}}$ and $\boldsymbol{Q_{DHN,mn,k,h}}$ are set equal to zero.

3.3.2. Electrical microgrid

For each electric line l (with $l = 1,2, \dots, L$) connecting two nodes n and m, the decision variables involved in the model of the electrical microgrid (EMG) are: the capacity of the network line ($\boldsymbol{C_{EMG,l,nm}}$) connecting the two nodes, in kW, the power flowing from node n to node m ($\boldsymbol{P_{EMG,nm}}$), in kW, and the power flowing from node m to node n ($\boldsymbol{P_{EMG,mn}}$), in kW. The power streams are bounded by the network line capacity, as shown in Eq. (18).

$$\boldsymbol{P_{EMG,nm,k,h}} + \boldsymbol{P_{EMG,mn,k,h}} \leq \boldsymbol{C_{EMG,l,nm}}. \quad (18)$$

If two nodes n and m are not connected by a EMG line, then $\boldsymbol{C_{EMG,l,nm}}$ is not defined, and $\boldsymbol{P_{EMG,nm,k,h}}$ and $\boldsymbol{P_{EMG,mn,k,h}}$ are set equal to zero.

3.4. Energy balances

Two energy balance constraints are imposed for each node, typical day, and time step of the typical day. The "+" sign is assigned to power/heat flows entering a node, the "–" sign to power/heat flows exiting a node.

Equation (19) shows the electrical energy (electricity) balance.

$$-D_{el,n,k,h} - \sum_m \boldsymbol{P_{EMG,nm,k,h}} + \sum_m \boldsymbol{P_{EMG,mn,k,h}}(1 - \lambda_{EMG}) - \boldsymbol{P_{exp,n,k,h}} + \boldsymbol{P_{imp,n,k,h}} - P_{HP,n,k,h} + P_{PV,n,k,h} + \boldsymbol{P_{ICE,n,k,h}} - \boldsymbol{P_{EES,chrg,n,k,h}} + \boldsymbol{P_{EES,disch,n,k,h}} = 0. \quad (19)$$

D_{el} is the hourly electricity demand in kW, m is the set of nodes connected to the node n, $\lambda_{EMG} = 0.02$ is the constant loss factor of the microgrid.

Equation (20) shows the thermal energy (heat) balance.

$$-D_{th,n,k,h} - \sum_m \boldsymbol{Q_{DHN,nm,k,h}} + \sum_m \left[\boldsymbol{Q_{DHN,mn,k,h}}\left(1 - len_{p,nm}\lambda'_{DHN}\right) - len_{p,nm}\lambda''_{DHN}\right] + \boldsymbol{Q_{HP,n,k,h}} + Q_{ICE,n,k,h} - \boldsymbol{Q_{TES,chrg,n,k,h}} + \boldsymbol{Q_{TES,disch,n,k,h}} = 0. \quad (20)$$

D_{th} is the hourly heating demand in kW, m is the set of nodes connected to the node n, len_p is the length of the pipeline in m, $\lambda'_{DHN} = 5.4 \times 10^{-5}\ 1/\mathrm{m}$ and $\lambda''_{DHN} = 7.4 \times 10^{-3}\ \mathrm{kW/m}$ are the linearization coefficients of the district heating losses calculated according to [9] as a function of the pipeline capacity and supply, return and ground temperatures ($T_{supply} = 70°\mathrm{C}$, $T_{return} = 40°\mathrm{C}$, and $T_{ground} = 10°\mathrm{C}$, respectively).

3.5. Objective function

The objective function f, to be minimized, represents the life cycle cost of the system actualized to one-year operation. f is composed of two contributions: f', associated with operation costs, and f'' associated with investment costs. Thus, $f = f' + f''$. f' and f'' are given in Eq. (21) and Eq.(22), respectively.

$$f' = \sum_k w_k \sum_n \sum_h \left[c_{gas}\left(F_{ICE,n,k,h} + F_{BOIL,n,k,h}\right) + c_{el,buy}\boldsymbol{P_{imp,n,k,h}} - c_{el,sell}\boldsymbol{P_{exp,n,k,h}}\right]. \quad (21)$$

$$f'' = \{\sum_n \sum_g [\tau_g (c_{inv,var,g} \boldsymbol{C_{g,n}} + c_{inv,fix,g})]\} + \{\sum_p [\tau_{DHN} len_p (c_{inv,var,DHN} \boldsymbol{C_{DHN,p,nm}} + c_{inv,fix,DHN})]\} + \{\sum_l [\tau_{EMG} len_l (c_{inv,var,EMG} \boldsymbol{C_{EMG,l,nm}} + c_{inv,fix,EMG})]\}. \quad (22)$$

w_k is the weight of the typical day k, $c_{gas} = 70€/\text{MWh}$ is the purchasing cost of natural gas, $c_{el,buy} = 200€/\text{MWh}$ is the purchasing cost of electricity from the national grid, and $c_{el,sell} = 50€/\text{MWh}$ is the selling price of electricity to the national grid. The subscript g (with g = PV, ICE, BOIL, HP, TES, EES) refers to the set of energy conversion and storage technologies; $c_{inv,var}$ and $c_{inv,fix}$ are the linearization coefficients of the investment cost of a technology or network (they are reported in Table 2 with their units); $\boldsymbol{C}$ is the capacity (decision variable); len refers to the length of a network branch in m; τ is the actualization factor of a technology or network and is calculated in Eq.(23), where $r = 0.05$ is the interest rate and a is the lifetime of a technology or network (see Table 2).

$$\tau = \frac{r(1+r)^a}{(1+r)^a+1}. \quad (23)$$

Note that operation and maintenance costs of the installed components are not shown in Eq. (22) for simplicity. However, they are included and calculated as a share of the investment cost.

Table 2 Linearized investment cost and lifetime of the energy conversion and storage technologies and energy networks.

Quantity	PV	ICE	BOIL	HP	TES	EES	DHN	EMG
$c_{inv,var}$	1250€/kW	1740€/kW	65€/kW	117€/kW	244€/kWh	880€/kWh	103€/kW/m	34€/kW/m
$c_{inv,fix}$	0€	32050€	1625€	2145€	970€	3495€	0.2€/m	0.05€/m
a, years	20	20	20	20	20	20	40	40

The function Φ defines the CO2 emissions of the system in one year of operation, as shown in Eq. (24).

$$\Phi = \sum_k w_k \sum_n \sum_h [e_{gas}(F_{ICE,n,k,h} + F_{BOIL,n,k,h}) + e_{el,grid} \boldsymbol{P_{imp,n,k,h}}]. \quad (24)$$

$e_{gas} = 197\text{kg/MWh}$ is the direct emission factor of natural gas, $e_{el,grid} = 356\text{kg/MWh}$ is the indirect emission factor associated with the electrical energy withdrawn from the national grid.

A reference scenario is defined by assuming that the aggregated electricity demand of the system is fulfilled by withdrawing electricity from the national grid, whereas the aggregated heating demand is met by burning natural gas in gas boilers. The resulting life cycle cost over one year of operation is $f_{ref} = 135.4\text{k€}$, whereas the CO2 emissions are $\Phi_{ref} = 307.6\text{ton}$.

A global constraint can be imposed on the maximum amount of CO2 emissions, in order to meet certain decarbonization targets. Equation (25) shows such a constraint, where $\varepsilon > 0$ is a fixed parameter.

$$\Phi \leq \varepsilon \times \Phi_{ref}. \quad (25)$$

By iteratively decreasing the value of ε, it is possible to carry out a sort of multi-objective optimization (the so-called ε-constrained multi-objective optimization) in order to obtain the Pareto front of the optimal solutions achieved for increasingly stricter reduction targets in carbon emissions.

4. Results

4.1. Cost-optimal system layout

Initially, the optimization model has been tested without imposing the constraint on CO2 emissions (Eq. (25)). Thus, the obtained results correspond to the cost optimal solution. The resulting value of the objective function, i.e., of the life cycle cost over one year, is $f = 124.3\text{k€}$, which is 8.2% lower than the reference scenario. The operation costs contribute for $f' = 52.1\text{k€}$, whereas the investment costs for $f'' = 72.7\text{k€}$. The total CO2 emissions over one year are $\Phi = 167.8\text{ton}$, which are 45.4% lower than the reference scenario. Hence, a sensible reduction in CO2 emissions results to be economically convenient even without imposing decarbonization targets.

Figure 2 shows the optimal layout of the energy networks, with the capacity of the district heating pipelines and electrical microgrid lines. Table 3 reports the optimal capacity of the energy conversion and storage plants at the node in which they are installed. The capacity of the DHN pipelines decreases by moving from the energy hub towards the end users. This is due to the mono-directionality of the heat flow, which only flows from the hub to the users. Note that the capacity of the DHN is higher than the one strictly required for meeting the heating demand of the end users because of the DHN losses, which have a not negligible impact on the system (79 MWh of losses in one year, more than 20% of the total heating demand). The installed capacity of PV is predominant, with 443.9 kW, for a yearly electricity production of 661.1 MWh that corresponds to a utilization factor of 17% (equivalent hours at the nominal power compared to the 8760 hours of one year). The

https://doi.org/10.52202/069564-0302

installed capacity of the ICE is 57.8 kW, for a yearly electricity production of 198.8 MWh corresponding to a utilization factor of 39%. The gas boiler allows covering the heating demand peaks. Its installed capacity is of 183 kW, for a yearly heat production of 43.6 MWh corresponding to a utilization factor of 3%. The HP covers the heating demand not covered by ICE and BOIL. Its installed capacity is 77.7 kW, for a yearly heat production of 134.2 MWh corresponding to a utilization factor of 20% The installed capacity of TES allows improving the operation flexibility of ICE and HP, thereby increasing their utilization factor. The installed capacity of EES is negligible. The electricity export to the national grid prevails on the electricity import because of the high capacity of PV. This is reflected by how the capacity of the electrical microgrid lines is distributed. In fact, it increases moving from the end users towards node 0, in which the system interfaces with the national grid.

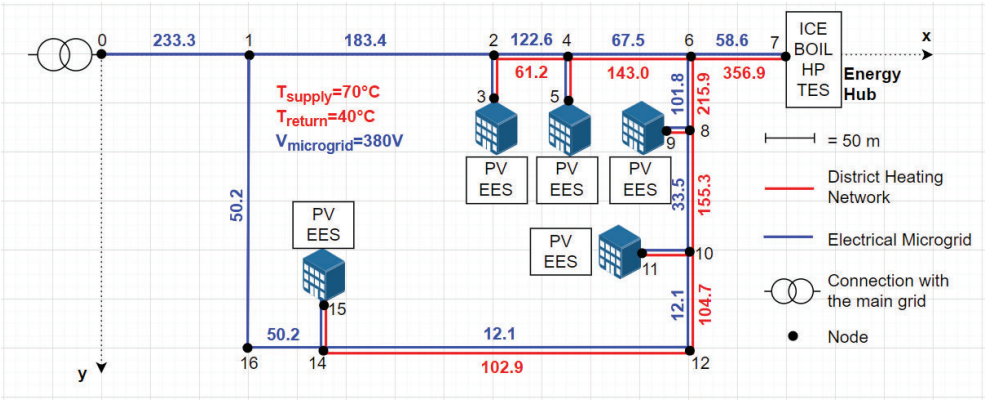

Figure 2 Cost-optimal layout of the energy networks. The capacities of the district heating pipelines and of the microgrid lines, in kW, are shown in red and blue, respectively.

Table 3 Capacity of the installed energy conversion and storage plants.

Node	PV, kW	ICE, kW	BOIL, kW	HP, kW	TES, kWh	EES, kWh
3	100.0	0	0	0	0	0.5
5	100.0	0	0	0	0	0.5
7	8.0	57.8	183.0	77.7	95.1	0
9	95.2	0	0	0	0	0.5
11	48.4	0	0	0	0	3.7
15	92.3	0	0	0	0	0.5

Figure 3 shows the energy balances (electricity and heat) of the whole system over one year, with a daily resolution. It is obtained by replacing each day of the year with the typical day representing it. The predominance, in terms of energy, of PV generation is clear, as also the prevalence of the electricity export compared to import. Globally, 77% of the total electricity demand is covered by electricity generated on site, whereas 37% of the generated electricity is exported. The ICE is more exploited during the cold season because of the contemporary need of electricity and heat by the end users, which makes more effective a CHP operation. The HP share on the daily generation of thermal energy is higher during the warm season, because of the high availability of “free of charge” electricity from PV. However, in absolute terms, the HP generates more in winter, when the heating demand is higher. The role of the boiler in covering the heating demand peaks is clear.

4.2. Variation of the reduction target on carbon emissions

The effect of imposing stricter reduction targets in CO_2 emissions has also been analysed. This corresponds to a decrease in the value of ε in Eq. (25), which represents the share of CO_2 emissions compared to the reference scenario. The cost-optimal system configuration, which does not consider that constraint, already implies a reduction in CO_2 emissions of 45%, corresponding to $\varepsilon = 0.55$. Thus, ε has been varied from 0.55 towards 0. Figure 4a shows the obtained Pareto front. It is evident that, starting from $\varepsilon = 0.55$, the minimization of the life cycle cost and the minimization of the carbon emissions are two contrasting objectives. Thus, reducing ε results in increasing the life cycle cost. It is possible to reduce the CO2 emissions until 120ton/year (60% reduction compared to the reference) while maintaining the economic effectiveness of the system with respect to the reference scenario. Accordingly, a further reduction of ε results in compromising the economic convenience of the proposed system. Moreover, CO_2 emissions cannot be reduced to zero because of the saturation of the PV and EES potentials (i.e., the available area for installing PV and space for installing EES become fully exploited). The minimum value that CO_2 emissions can reach is 69 ton/year, 78% less than in the reference scenario. However, the corresponding life cycle cost is 45% higher than the cost-optimal case.

Figure 4b shows how the capacity of the installed energy conversion and storage plants and largest network branches (EMG line 0-1, DHN pipeline 6-7) varies with ε, i.e., with decreasing CO_2 emissions (the plot should be read from right to left). The most evident result is the progressive increase in PV, HP, EES and EMG capacities. Moving from the cost-optimal system configuration to the minimum emitting one, the PV capacity almost doubles, the HP capacity increases of 130%, the EES capacity increases of more the 100 times, and the EMG capacity increases of 85%. The reason is that PV is the only renewable-based technology available. Thus, the increase in PV capacity is accompanied by an increase in HP capacity, in order to decarbonize the heating demand, and an increase in EES capacity, in order to decarbonize the electricity demand during the hours in which PV generation is not available. The EMG capacity increases too, in order to accommodate the increasing generation surplus from PV. The boiler capacity slowly decreases with decreasing ε. The ICE capacity remains more or less constant, except for a sharply decrease (-91%) to allow the last marginal reduction in CO2emissions. This reflects a sharply increase (+93%) in TES capacity, which is required to improve the flexibility of the HP and, in turn, its utilization factor. The DHN capacity remains constant.

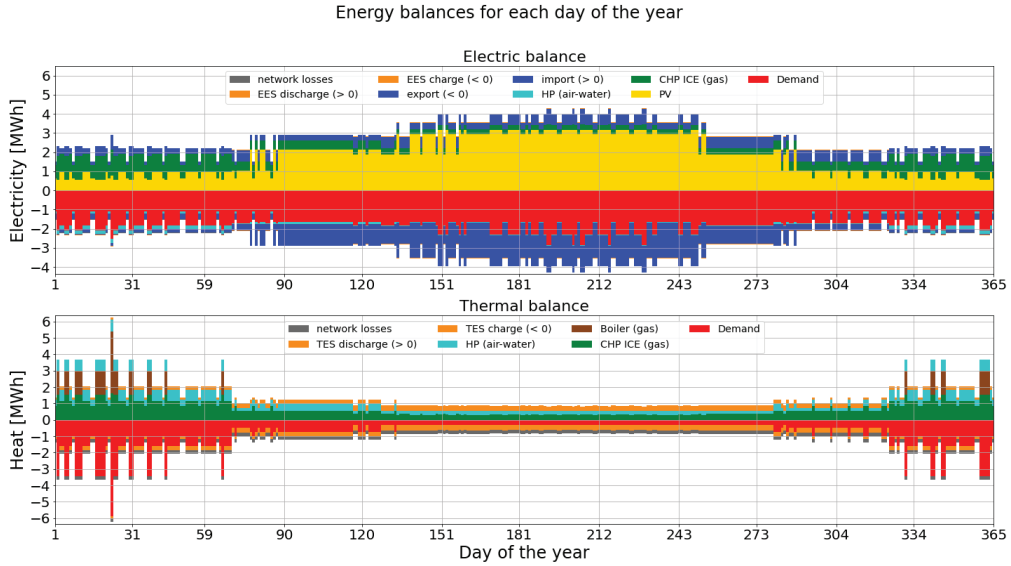

Figure 3 Yearly energy balances of the considered multi energy system with a daily resolution.

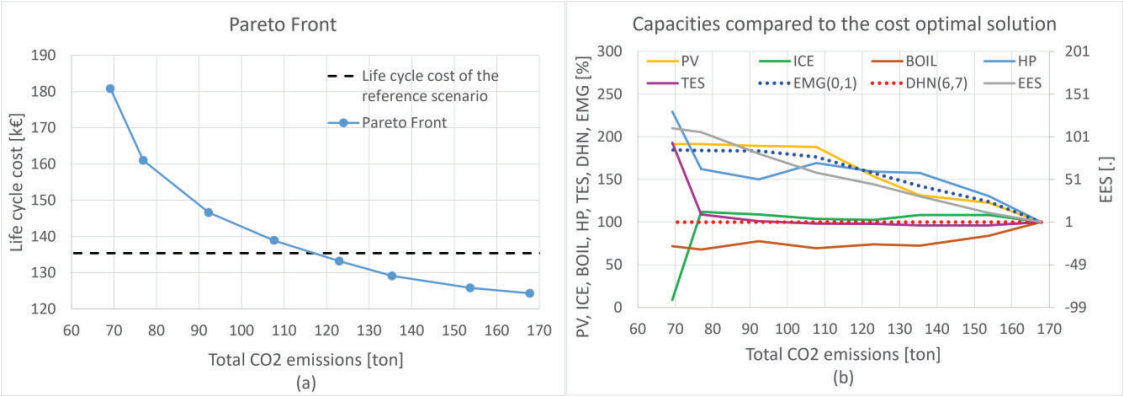

Figure 4 Results of the optimization for increasingly stricter constraints on CO2 emissions: a) Pareto front and b) share of the installed capacities compared to the cost-optimal solution.

5. Conclusions

This paper presents a general method for the design and operation optimization of multi-energy systems integrated with energy networks, with the goal of defining cost-effective system configurations to meet increasingly stricter decarbonization targets. The proposed method makes it possible to concurrently optimize the capacity of the available energy conversion and storage plants, the capacity of each branch of the available networks, and their operation, in order to minimize the life cycle cost of the system for a given cap on carbon

https://doi.org/10.52202/069564-0302

emissions. A district multi-energy system composed of residential and commercial buildings, with their electricity and heating demands, and including a district heating network and an electrical microgrid has been considered as a test case. Without imposing any constraints on CO2 emissions, results show that it is possible to reduce the carbon emissions of the system of 45%, while also decreasing the life cycle cost of 8%, with respect to a reference scenario in which the entire electricity demand is fulfilled by withdrawing electricity from the national grid and the entire heating demand is met by burning natural gas in gas boilers. However, a further decarbonization compromises the cost-effectiveness of the system because of the investments in carbon-neutral technologies and electrical microgrid, the installed capacity of which steeply increases.

The main findings of the study are summarized below.

- Photovoltaic is a promising solution for decarbonizing the electricity demand, by contributing for more than 75% to the total electricity generation. Electrical storage systems are necessary for a deep decarbonization.
- The higher share of photovoltaic generation in deeply decarbonized scenarios requires increasing the capacity of the electrical microgrid up to 85% compared to the cost-optimal system configuration.
- The economic convenience of distributed electricity generation is mainly due to the self-consumption, which approaches 80% of the electricity demand, rather than to selling energy to the national grid.
- Heat pumps are very effective in decarbonizing the heating demand if a surplus of photovoltaic generation is available on site. Their contribution to the thermal power generation approaches 100% in deeply decarbonized scenarios. Moreover, thermal energy storage allows improving their utilization factor.
- Gas-fuelled combined heat and power internal combustion engines can contribute to the decarbonization of both electricity and heating demand in a first phase. However, the scarce heating demand of commercial-residential districts during the warm season sensibly worsens the utilization factor of this technology, which results to be lower than 40%.
- The capacity of the considered tree-shaped district heating network depends only on the heating demand of the end users, thereby remaining unchanged when the decarbonization target varies.

The proposed paper is intended as a part of a wider study aiming at defining a method for the complete synthesis, design and operation optimization of multi energy systems integrated with energy networks. This means that the present work will be further developed in order to include the synthesis of the networks' topology, the selection of the number and type of the energy conversion and storage plants, and their siting within the system into the optimization problem. The idea is to solve the overall synthesis, design and operation problem by means of an evolutionary algorithm, in which the method proposed here is run many times at each iteration for different configurations of the networks' topology and plants' position.

Acknowledgments

The Authors thank "Fondazione Ing. Aldo Gini" of the University of Padova for the economic support.

Project financially supported by BIRD 2019 Research Program of University of Padova (Project BIRD197944)

Nomenclature

Abbreviations

DHN District heating network

EMG Electrical microgrid

MES Multi-energy system

SDO Synthesis, design and operation

Subscripts

g energy conversion and storage technologies (with g = PV, ICE, BOIL, HP, TES, EES)

h hours of the day (with h = 1, 2, …, 24)

k typical days or cluster centers (with k = 1, 2, …, 10)

l electrical microgrid lines (with l = 1, 2, …, 16)

n nodes of the system (with n = 0, 1, …, 16) (alternatively, m)

p district heating pipelines (with p = 1, 2, …, 12)

References

[1] E. Papadis and G. Tsatsaronis, "Challenges in the decarbonization of the energy sector," *Energy,* vol. 205, p. 118025, 2020. https://doi.org/10.1016/j.energy.2020.118025.

[2] P. Mancarella, "MES (multi-energy systems): An overview of concepts and evaluation models," *Energy,* vol. 65, pp. 1-17, 2014. https://doi.org/10.1016/j.energy.2013.10.041.

[3] G. Volpato, G. Carraro, M. Cont, P. Danieli, S. Rech, and A. Lazzaretto, "General guidelines for the optimal economic aggregation of prosumers in energy communities," *Energy,* vol. 258, p. 124800, 2022. https://doi.org/10.1016/j.energy.2022.124800.

[4] C. A. Frangopoulos, "Recent developments and trends in optimization of energy systems," *Energy,* vol. 164, pp. 1011-1020, 2018. https://doi.org/10.1016/j.energy.2018.08.218.

[5] H. Lund, P. A. Østergaard, T. B. Nielsen, S. Werner, J. E. Thorsen, O. Gudmundsson*, et al.*, "Perspectives on fourth and fifth generation district heating," *Energy,* vol. 227, p. 120520, 2021.

[6] B. Leitner, E. Widl, W. Gawlik, and R. Hofmann, "A method for technical assessment of power-to-heat use cases to couple local district heating and electrical distribution grids," *Energy,* vol. 182, pp. 729-738, 2019. https://doi.org/10.1016/j.energy.2019.06.016.

[7] M. Nazari-Heris, B. Mohammadi-Ivatloo, and S. Asadi, "Optimal operation of multi-carrier energy networks with gas, power, heating, and water energy sources considering different energy storage technologies," *Journal of Energy Storage,* vol. 31, p. 101574, 2020. https://doi.org/10.1016/j.est.2020.101574.

[8] B. Talebi, P. A. Mirzaei, A. Bastani, and F. Haghighat, "A Review of District Heating Systems: Modeling and Optimization," *Frontiers in Built Environment,* vol. 2, 2016. 10.3389/fbuil.2016.00022.

[9] J. Röder, B. Meyer, U. Krien, J. Zimmermann, T. Stührmann, and E. Zondervan, "Optimal Design of District Heating Networks with Distributed Thermal Energy Storages – Method and Case Study," *International Journal of Sustainable Energy Planning and Management,* vol. 31, pp. 5-22, 2021. 10.5278/ijsepm.6248.

[10] S. Rech and A. Lazzaretto, "Smart rules and thermal, electric and hydro storages for the optimum operation of a renewable energy system," *Energy,* vol. 147, pp. 742-756, 2018. https://doi.org/10.1016/j.energy.2018.01.079.

[11] L. M. P. Ghilardi, A. F. Castelli, L. Moretti, M. Morini, and E. Martelli, "Co-optimization of multi-energy system operation, district heating/cooling network and thermal comfort management for buildings," *Applied Energy,* vol. 302, p. 117480, 2021. https://doi.org/10.1016/j.apenergy.2021.117480.

[12] E. Dal Cin, G. Carraro, G. Volpato, A. Lazzaretto, and P. Danieli, "A multi-criteria approach to optimize the design-operation of Energy Communities considering economic-environmental objectives and demand side management," *Energy Conversion and Management,* vol. 263, p. 115677, 2022. https://doi.org/10.1016/j.enconman.2022.115677.

[13] M. Wirtz, "nPro: A web-based planning tool for designing district energy systems and thermal networks," *Energy,* vol. 268, p. 126575, 2023. https://doi.org/10.1016/j.energy.2022.126575.

[14] M. Wirtz, M. Heleno, A. Moreira, T. Schreiber, and D. Müller, "5th generation district heating and cooling network planning: A Dantzig–Wolfe decomposition approach," *Energy Conversion and Management,* vol. 276, p. 116593, 2023. https://doi.org/10.1016/j.enconman.2022.116593.

[15] S. Mashayekh, M. Stadler, G. Cardoso, and M. Heleno, "A mixed integer linear programming approach for optimal DER portfolio, sizing, and placement in multi-energy microgrids," *Applied Energy,* vol. 187, pp. 154-168, 2017. https://doi.org/10.1016/j.apenergy.2016.11.020.

[16] E. D. Mehleri, H. Sarimveis, N. C. Markatos, and L. G. Papageorgiou, "A mathematical programming approach for optimal design of distributed energy systems at the neighbourhood level," *Energy,* vol. 44, pp. 96-104, 2012. https://doi.org/10.1016/j.energy.2012.02.009.

[17] E. D. Mehleri, H. Sarimveis, N. C. Markatos, and L. G. Papageorgiou, "Optimal design and operation of distributed energy systems: Application to Greek residential sector," *Renewable Energy,* vol. 51, pp. 331-342, 2013. https://doi.org/10.1016/j.renene.2012.09.009.

[18] M. Casisi, S. Costanzo, P. Pinamonti, and M. Reini. (2019, Two-Level Evolutionary Multi-objective Optimization of a District Heating System with Distributed Cogeneration. *Energies 12(1),* DOI: *10.3390/en12010114*.

[19] P. Gabrielli, M. Gazzani, E. Martelli, and M. Mazzotti, "Optimal design of multi-energy systems with seasonal storage," *Applied Energy,* vol. 219, pp. 408-424, 2018.

[20] M. Hoffmann, L. Kotzur, D. Stolten, and M. Robinius. (2020, A Review on Time Series Aggregation Methods for Energy System Models. *Energies 13(3)*.

[21] S. Rech, "Smart Energy Systems: Guidelines for Modelling and Optimizing a Fleet of Units of Different Configurations," *Energies,* vol. 12, p. 1320, 2019. doi:10.3390/en12071320.

[22] L. Kotzur, P. Markewitz, M. Robinius, and D. Stolten, "Time series aggregation for energy system design: Modeling seasonal storage," *Applied Energy,* vol. 213, pp. 123-135, 2018. https://doi.org/10.1016/j.apenergy.2018.01.023.

[23] F. Glover, "Improved Linear Integer Programming Formulations of Nonlinear Integer Problems," *Management Science,* vol. 22, pp. 455-460, 1975. http://www.jstor.org/stable/2630109